Demonstration of photonic neural network for fiber nonlinearity compensation in long-haul transmission systems

Chaoran Huang[1*] Shinsuke Fujisawa[2*], Thomas Ferreira de Lima[1], Alexander N. Tait[1,†], Eric Blow[1], Yue Tian[2], Simon Bilodeau[1], Aashu Jha[1], Fatih Yaman[2], Hussam G. Batshon[2], Hsuan-Tung Peng[1], Bhavin J. Shastri[1,3], Yoshihisa Inada[4], Ting Wang[2] and Paul. R. Prucnal[1]

[1]Princeton University, Princeton, NJ 08542, USA
[2]NEC Laboratories America, Inc.,4 Independence Way, Princeton, NJ 08540, USA
[3]Queen's University, Kingston, ON K7L 3N6, Canada
[4]Submarine Network Division, NEC Corporation, 108-8001 Tokyo, Japan
[†]Now at National Institute of Standards and Technology, Boulder, CO 80305, USA
Corresponding authors' email addresses: chaoranh@princeton.edu, sfujisawa@nec-labs.com
** These authors equally contributed to this work*

Abstract: We demonstrate the experimental implementation of photonic neural network for fiber nonlinearity compensation over a 10,080 km trans-pacific transmission link. Q-factor improvement of 0.51 dB is achieved with only 0.06 dB lower than numerical simulations.

1. Introduction

The potential benefits of artificial neural networks (ANNs) have recently been demonstrated for optical fiber communication, such as fiber nonlinearity compensation (NLC) in long-haul transmission systems [1]. Benefiting from the training and execution procedures of ANNs, ANN-NLC algorithms can create effective fiber transmission models from the received symbols without needing prior knowledge of transmission link parameters. Compared with the deterministic NLC approaches, such as digital back propagation [2,3] and single step perturbation method [4], ANN-NLC provides comparable system performance with lower computational complexity. However, despite the reduced complexity with ANN-NLC, the hardware implementation of real-time ANN-NLC for high-speed optical transmission systems is still a challenge with conventional electronics (e.g. ASIC), considering the required computation speed and associated power consumption.

Applications such as ANN-NLC for optical communications demand for low-power and high-speed neural network implementation, and therefore necessitates the investigation of new hardware beyond purely electronic physics. Photonic neural networks (PNNs) combine the high speed of photonic devices with highly parallel optical interconnects that have originally been developed for telecommunications [5,6]. This makes PNNs naturally suitable for processing high-speed optical communication signals. Our prior research on PNN has revealed the analogy between the neural networks and wavelength division multiplexing (WDM) photonic hardware and demonstrated underlying on-chip devices that allow practical implementation on silicon photonic platforms [7,8]. The advances of silicon photonics enable integrations of optical devices and interconnects with sufficient density to perform computing tasks driven by real-world applications [9].

In this paper, we report the experimental results of employing PNN for fiber nonlinearity compensation for a 10,080 km trans-Pacific optical transmission system. We demonstrate that the PNN effectively compensates the nonlinear transmission impairment and achieves Q-factor improvement of 0.51 dB. Significantly, the experimentally obtained Q-factor improvement is only 0.06 dB lower compared to numerical simulations of ANN-NLC algorithm with the same neural network architecture. The superior precision of PNN demonstrates the feasibility of using PNN for optical fiber transmission applications.

2. ANN-NLC and photonic neural network implementation

The ANN model shown in Fig. 1 (a) is optimized for transmission nonlinearity compensation [1]. The fully-connected feedforward neural network consists of an input layer with triplets accounting for intra-channel nonlinear distortion, two hidden layers with two and eight neurons, respectively, and two output neurons corresponding to the real and imaginary parts of the nonlinear distortion. The estimated nonlinearity is subtracted from the received symbols of interest before being sent to FEC decoding.

In this experiment, we demonstrate the concept of implementing ANN-NLC using PNN on a silicon photonic chip. We implement the functionality of the second hidden layer which consists of eight neurons and each neuron is connected to the two outputs from the first layer with off-line trained weight configurations. Fig. 1 (b) shows the micrograph of one photonic neuron connected to a microring (MRR) weight bank. The MRR weight bank provides the key functionality to configure connection strengths in the analog WDM network. The weight (ranging from -1 to 1) on each MRR is determined by how much power of a given WDM channel is split between 2 ports of a balanced photodetector (BPD), as shown in Fig. 1 (b). The detected signal drives an MRR modulator, of which the nonlinear transmission function serves as the activation function of a neuron. The on-chip inductor and capacitor provide network matching circuit for efficient optical-electrical-optical (OEO) conversion.

The experimental setup is illustrated in Fig. 1(c). As shown in Fig. 1 (a), the second hidden layer takes the two neurons' outputs from the first hidden layer. Hence, we generate two optical signals each encoded with a neuron output to emulate the first hidden layer outputs. The data waveforms of the first layer outputs are obtained from neural network simulations and are modulated on two WDM lasers by the Mach-Zehnder modulators driven by an arbitrary waveform generator (AWG). The modulated signals are combined and then are coupled into the PNN chip through grating couplers shown in Fig. 1 (d) [6]. Inside the PNN, the two signals are first weighted by the MRR weight bank and then detected by the BPD. The neuron CW laser pump is coupled into the PNN chip and is modulated by the photocurrent generated from the weighted signals. The modulator's p-n junction is forward biased to achieve a high modulation efficiency [10]. The neuron's output is coupled off-chip, detected, and sampled by a real-time oscilloscope.

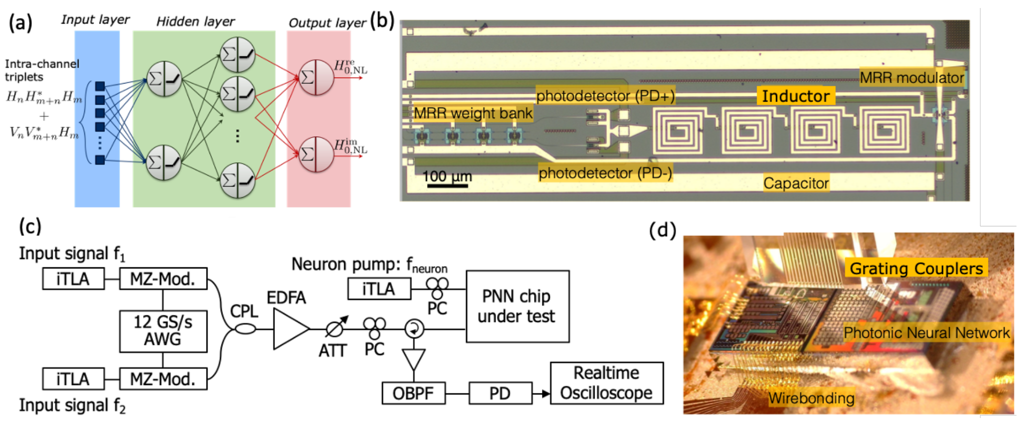

Fig. 1: (a) Schematic of ANN-NLC structure; (b) Micrograph of a photonic neuron and MRR weight bank; (c) Experimental setup; (d) Image of the PNN chip under test and experimental setup for optical coupling and wire bonding.

3. Demonstration of Photonic Neural Network for Fiber Nonlinearity Compensation

To demonstrate the PNN for fiber nonlinearity compensation, the NLC model needs to be trained based on the activation function of the photonic neurons. We first characterize the activation function by sending a training data pattern to the photonic neuron modulator and comparing it with the corresponding neuron output. The input and output signals (as depicted in Fig. 2 (a)) are captured using the real-time oscilloscope. Fig. 2 (b) shows the normalized activation function at a neuron pump frequency of 194.776 THz. The full-scale activation function is reconstructed from each snapshot generated at different neuron pump frequencies and fit to a Lorentzian function.

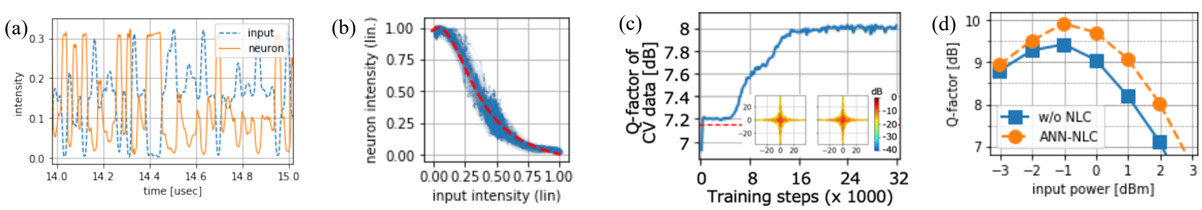

Fig. 2: (a) Waveforms of a training pattern and the corresponding neuron output captured by a real-time oscilloscope; (b) A snapshot of the activation function of a photonic neuron modulator at f_{neuron} = 194.776 THz with Lorentzian fitting (dotted line) (c) ANN-NLC training convergence with a Lorentzian activation function (inset: density plot of the input layer weights of the ANN-NLC model with 821 triplets); (d) Transmission performance for an execution frame of a 32 Gbaud PM-16QAM signal over a 10,080 km PSCF transmission link.

Next, we apply the Lorentzian activation function to the NLC model (Fig. 1 (a)), and train the neural network with received symbols of a single channel 32 Gbaud PM-16QAM signal over a 10,080 km pure silica core fiber (PSCF) transmission link, with 60 km span length and EDFA-only amplification, obtained by VPItransmissionMaker simulations. As the training proceeded, the Q-factor of the cross-validation (CV) data at the input power of 2 dBm is steadily increased and then converged as shown in Fig. 2 (c). Therefore, the NLC model is successfully converged with the Lorentzian activation function. Fig. 2 (d) illustrates the Q-factor improvement obtained from the trained NLC applied to an execution frame of 32,106 symbols under the same transmission condition. We observe 0.57 dB Q-factor improvement at the optimal input power of -1 dBm.

Based on the weights and biases of the trained NLC model, we configure each MRR weight and neuron bias such that the PNN functions as the NLC model. Fig. 3 (a) shows snapshots that compare each neuron output from the ANN-NLC simulation and that from PNN within 1-μsec interval. The mean square error (MSE) for each neuron is calculated over the execution frame. The evaluated MSE, ranging from 2.59 % to 4.40 %, indicates that the PNN provides high accuracy. Fig. 3 (b) illustrates the error distributions of the neuron1 (the worst MSE) and the neuron 2 (the best MSE), both of which approximately correspond to a Gaussian distribution. Furthermore, we evaluate the Q-factor of the transmission signals reconstructed from the eight photonic neuron outputs. Fig. 3 (c) shows the constellation of the execution frame by the ANN-NLC numerical simulation, corresponding to 0.57 dB Q-factor improvement, whereas the constellation of the same execution frame measured from the PNN output is plotted in Fig. 3 (d), achieving 0.51 dB Q-factor improvement. The Q-factor improvement of PNN-NLC is only degraded by 0.06 dB compared to the numerical simulation of ANN-NLC, which further confirms the superior precision of PNN.

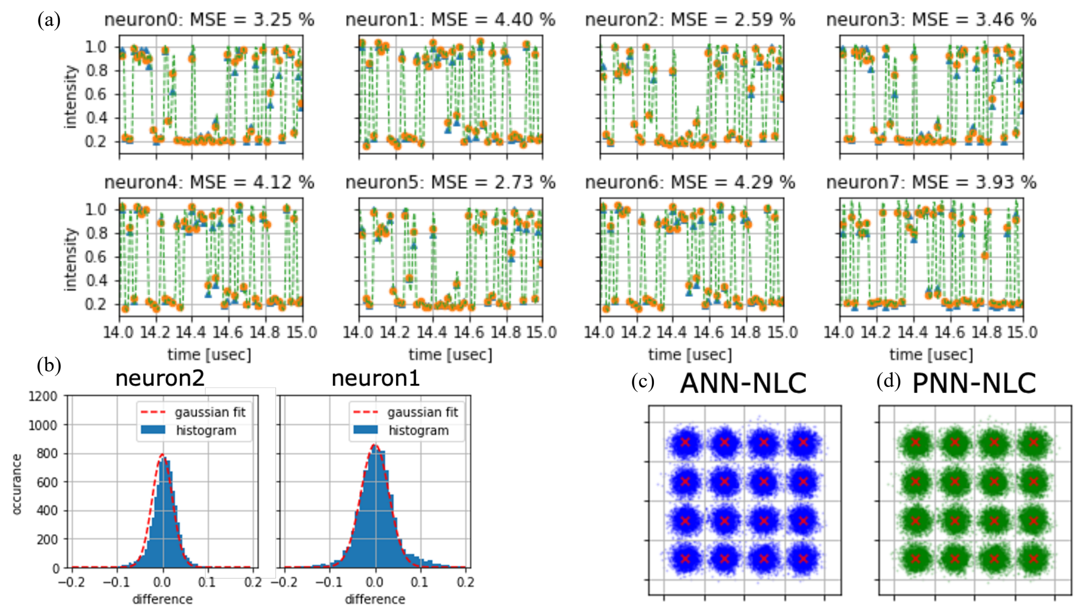

Fig. 3: (a) Comparison of each neuron output between ANN-NLC and PNN-NLC (blue triangle: ANN-NLC, orange dot: PNN-NLC, green dotted line: PNN neuron waveform); (b) error distributions of neuron 1 and 2; Constellations of X-polarization of a 32 Gbaud PM-16QAM, with the ANN-NLC gain of 0.57 dB in Q-factor (c) and with the PNN-NLC gain of 0.51 dB in Q-factor (d).

4. Conclusion

We have demonstrated the experimental implementation of PNN to compensate the fiber nonlinearity over a 10,080 km trans-Pacific transmission link of 32 Gbaud PM-16QAM signals. By utilizing PNN, we have achieved Q-factor improvement of 0.51 dB, which is only 0.06 dB lower than implementing the ANN with numerical simulation. The superior precision of PNN implies the feasibility of implementation of ANN-enabled signal processing for optical fiber communications on PNNs. Although the photonic neuron bandwidth of our current chip is limited, caused by the low extinction ratio of its MRR modulator, it can be realistically increased to accommodate the high-speed communication signals in future iterations [11]. Given such bandwidths, PNN will allow real-time ANN-enabled signal processing for high-speed communication signals with a single pipeline.

Acknowledgement

Defense Advanced Research Projects Agency (HR-00111990049); National Science Foundation (ECCS-1642962).

References

[1] S. Zhang *et al.*, Nature Communications **10,** 3033 (2019).
[2] E. Ip *et al.*, JLT **26**, pp. 3416-3425 (2008).
[3] X. Li *et al.*, Optics Express **16**, pp. 880-888 (2008).
[4] Z. Tao *et al.*, JLT **29**, pp 2570-2576 (2011).
[5] P. R. Prucnal *et al.*, *Neuromorphic Photonics* (CRC Press, 2017).
[6] T. F. de Lima *et al.*, manuscript in preparation.
[7] A. N. Tait *et al*. Scientific Reports **7**, 7430 (2017).
[8] A. N. Tait *et al.*, Phys. Rev. Appl. **11**, 064043 (2019).
[9] T. F. de Lima *et al.*, JLT **37**, pp. 1515-1534 (2019).
[10] Q. Xu *et al.*, Optics Express **15**, pp. 430-436 (2007).
[11] K. Nozaki *et al.*, Nature Photonics **13**, pp. 454-459 (2019).